

## Spectroscopic diagnostics and silicon cluster formation in silane plasmas

Yeonwon Kim<sup>†</sup>

(Received November 20, 2019 ; Revised March 5, 2020 ; Accepted April 22, 2020)

**Abstract:** We investigated the correlation of the slope of the Si\* intensity versus the SiH\* intensity with the Si cluster volume fraction. The light emitted from the plasma was analyzed using optical emission spectroscopy. The deposition rates with cluster and those of without clusters were measured using quartz crystal microbalances installed in the plasma reactor. The silicon cluster volume fraction was derived by comparing the resulting deposition rates with cluster and without clusters. The results showed that the slope of the Si\* intensity versus SiH\* intensity varied depending on the reaction conditions and was roughly correlated with the silicon cluster volume fraction. Therefore, this simple spectroscopic comparison could be used as an indicator of cluster incorporation into thin films.

**Keywords:** Plasma, Clusters, Thin film, QCM, OES

### 1. Introduction

Energy conservation and emissions reduction have become major issues in the shipping industry. In particular, since the energy efficiency design index (EEDI) and ship energy efficiency management plan (SEEMP) were added to the international convention for the prevention of pollution from ships (MARPOL) in 2011, many shipping countries have made great efforts to develop green ships utilizing renewable energy sources such as wind, solar, and biomass energy [1]. Among them, solar ships are emerging as a promising alternative in the rapidly developing green shipping industry [2]-[4].

Thin films of hydrogenated amorphous silicon (a-Si:H) are commonly used in thin film photovoltaic devices due to their relatively low material consumption, thicknesses of less than ~1  $\mu\text{m}$ , and potential for large-area production [5][6]. In particular, the use of reactive plasmas generated using radio frequency is the most common method of thin film deposition, as it provides flexibility in the choice of substrate (such as glass or polymers) due to the low process temperature, easy band-gap tuning, and the ability to stack multiple materials without critical damage.

However, light-induced degradation of the resulting devices, which is also known as the Staebler-Wronski effect (SWE), limits their performance [7]. The breakage of weak Si-Si bonds via light exposure can result in an increase in dangling bonds, which reduces the photo- and dark conductivity of the films [8].

One strategy to suppress the degradation of metastable a-Si:H is to reduce the polymerization of particles in the plasma gas phase reactions [9][10]. Many research groups have reported that suppressing the incorporation of particles during film deposition improves the optical and electrical properties of the film by reducing the amount of dangling bond defects on the surface of the growing film.

A great deal of research into the kinetics of particle growth and the incorporation of particles into the growing film has been conducted. Several research groups have reported that silicon particulates can grow in plasmas as a negatively charged state and subsequently be incorporated into the growing film. These particles may be produced during the continuous plasma processing and/or at the end of the process when the plasma is switched off [11]. During plasma discharge, the silicon particles are continuously negatively charged due to their larger cross-section and lower mobility compared to the fast-moving electrons [12][13]. Charged particles with a size of a several nanometers are electrostatically trapped in a localized region at the plasma/sheath boundary due to the balance between the opposing electrostatic and ion drag forces. As the size and mass of the particles increases, the force of gravity pulls the particles down onto the substrate. The particles can also be exposed to a low-electron-density region resulting from temporal plasma fluctuations; the negatively charged particles are then partially

<sup>†</sup> Corresponding Author (ORCID: <https://orcid.org/0000-0001-5638-4339>): Professor, Division of Marine Mechatronics, Mokpo National Maritime University, 91 Haeyangdaehak-ro, Mokpo-si, 58628, Jeollanam-do, Republic of Korea, E-mail: k.yeonwon@mmu.ac.kr, Tel: 061-240-7237

This is an Open Access article distributed under the terms of the Creative Commons Attribution Non-Commercial License (<http://creativecommons.org/licenses/by-nc/3.0>), which permits unrestricted non-commercial use, distribution, and reproduction in any medium, provided the original work is properly cited.

neutralized and fall onto the substrate. Particle transport and behavior in the post-plasma regime are also important [14]. When the plasma is switched off, the electric field rapidly decays, releasing the particles from the electrostatic trap; they are then rapidly neutralized by agglomeration among themselves and deposited on the film surface.

The particle agglomeration of silane radicals is related to the electron temperature of the bulk plasma. Highly reactive  $\text{SiH}_2$  radicals, which are known to trigger agglomeration, are easily generated at high electron temperatures ( $T_e > 9.47$  eV) [15].

$\text{SiH}_2$  radicals react with  $\text{Si}_n\text{H}_{2n+2}$  species with a high probability to form polymerized species. Notably, several research groups have reported that plasma reactors with decreased electron temperature (e.g., remote plasma reactors) lead to stable a-Si:H films with low Si cluster incorporation. However, the correlation between plasma emission characteristics and silicon cluster volume fraction ( $V_f$ ) in the resulting films is not yet fully understood. In the present work, the electron temperature is discussed by comparing the line intensities of  $\text{Si}^*$  ( ${}^1\text{P}^0$ , 288.2 nm) and  $\text{SiH}^*$  ( $\text{A}^2\Delta$ , 412.7 nm) under various conditions. The plasma characteristics measured using optical emission spectroscopy (OES) and the deposition rates obtained using quartz crystal microbalances (QCMs) are considered, and the  $V_f$  of Si clusters deposited at different working pressures are discussed in terms of the results.

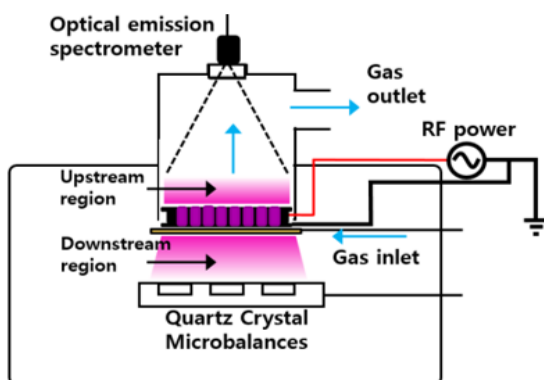


**Figure 1:** Multi-hollow plasma discharge reactor equipped with QCMs and OES

## 2. Experimental method

The experiments were conducted using a multi-hollow plasma discharge reactor, as shown in **Figure 1**. Plasma was generated using radio frequency (RF) energy in each hole of the multi-hole electrode. The source gases were introduced through a ring-shaped tube line placed around the electrode and flowed

toward the upstream region. The upward gas flow transported particles upstream and suppressed downstream particle diffusion. The experiments were conducted under a 30 sccm flow of  $\text{SiH}_4$  and at a pressure of 0.5 Torr using capacitively coupled RF discharge. The distance between the multi-hollow electrode and the QCMs was approximately 50 mm, and the laser passed through 20 mm below the electrode. The temperature of the QCMs was maintained at 100 °C.

The QCMs (Stanford Research QCM200) were placed in the upstream region to observe the deposition rate and the  $V_f$  values of the Si clusters. The details of the measurement technique are described elsewhere [16][17]. The plasma emission was observed using OES (Ocean Optics USB200+) through the upper quartz glass port. The intensities of  $\text{Si}^*$  and  $\text{SiH}^*$  were measured, and the relationship between the change in their intensities and the  $V_f$  of silicon clusters was analyzed.

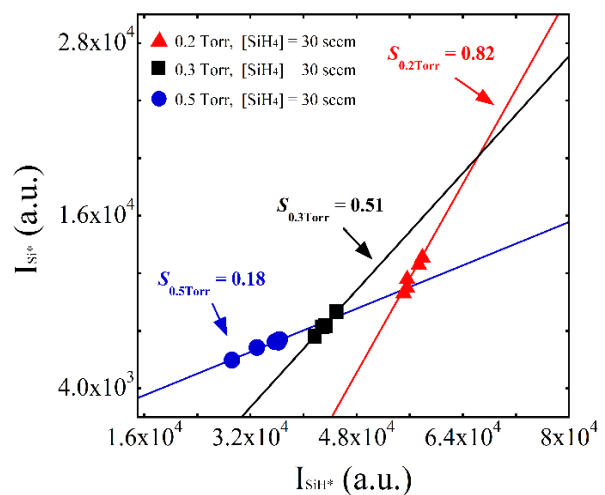


**Figure 2:** Slope of the  $\text{Si}^*$  intensity versus the  $\text{SiH}^*$  intensity at working pressures of 0.2, 0.3, and 0.5 Torr

## 3. Results and discussion

To investigate the changes in plasma emission with increasing working pressure, the intensity of the light emitted from the plasma discharge was measured using OES.  $\text{Si}^*$  and  $\text{SiH}^*$  have been reported to exhibit similar emission cross-section trends; thus, their intensity ratio can be used to predict the profile of the electron energy distribution function (EEDF). Namely, a higher  $\text{Si}^*/\text{SiH}^*$  ratio indicates a lower slope at the energy tail of the EEDF, which eventually leads to a higher electron temperature by modifying the EEDF profile [18]. Here, we have plotted the slope of the intensity ratio  $S$  ( $\Delta\text{Si}^*/\Delta\text{SiH}^*$ ), rather than the  $\text{Si}^*/\text{SiH}^*$  intensity ratio under a particular plasma condition.

$\Delta Si^*/\Delta SiH^*$  indicates the slope of the change in the  $SiH^*$  intensity versus the change in the  $Si^*$  intensity over a range of conditions, whereas  $Si^*/SiH^*$  represents the value under one specific plasma condition. The  $\Delta Si^*/\Delta SiH^*$  values were measured under different pressure conditions, and are plotted in **Figure 2**. The fitting lines connecting the filled triangles, squares, and circles indicate the dependence of the  $Si^*$  intensity on the  $SiH^*$  intensity at 0.2, 0.3, and 0.5 Torr, respectively. These measurements were performed under pure silane conditions with increasing applied voltage. The increase in the slopes of the solid trend-lines with decreasing pressure was related to the increase in electron temperature resulting from the longer mean free path under low pressure conditions, leading to formation of Si clusters in the plasma. These results show that the working pressure affected the plasma emission characteristics as well as the electron temperature.

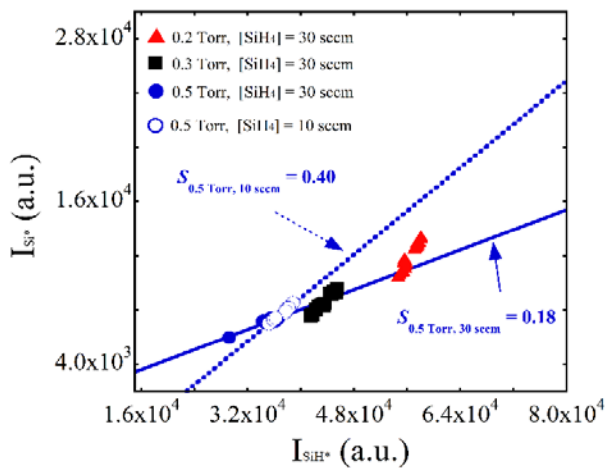


**Figure 3:** Effect of decreasing the gas flow rate on the slope of the  $Si^*$  intensity versus the  $SiH^*$  intensity

To investigate the effect of gas flow rate on  $\Delta Si^*/\Delta SiH^*$ , which was representative of the effective electron temperature, we plotted the slopes obtained at 30 sccm (solid line) together with that obtained at 10 sccm (dotted line) and 0.5 Torr. As shown in **Figure 3**, the slope increased from 0.18 to 0.40 when the gas flow rate was decreased from 30 sccm to 10 sccm. This might have been due to the longer gas residence time in the plasma region; i.e., because the source gases required more time to pass through the plasma region, they absorbed more power to decompose the gases into radical species, which typically occurs in the holes of the powered electrode. Highly reactive radicals such as  $SiH_2$ , which is a potential particle source, could also accumulate and agglomerate in the plasma region.

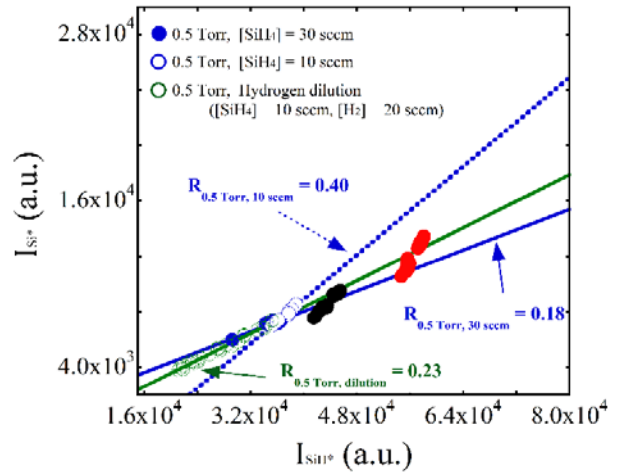


**Figure 4:** Effect of hydrogen dilution on the slope of the  $Si^*$  intensity versus the  $SiH^*$  intensity

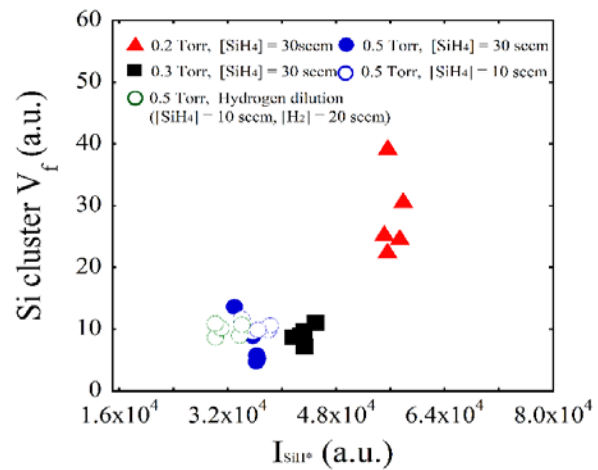


**Figure 5:** Variation in the silicon cluster volume fraction as a function of the  $SiH^*$  intensity

To determine the effect of hydrogen dilution on the plasma composition, the intensity of  $Si^*$  versus the intensity of  $SiH^*$  under hydrogen-diluted conditions was measured and is plotted together with relevant data from the pure silane experiments in **Figure 4**. The dotted line indicates the slope of the intensities of  $Si^*$  versus that of  $SiH^*$  under the pure silane condition; as shown, the slope decreased to 0.23 under hydrogen-diluted conditions. This result suggested that hydrogen dilution had an effect on the electron temperature [19]. Since Guha *et al* reported the formation of silicon films with high stability against light-induced degradation using hydrogen dilution techniques, many studies have been conducted to determine the role of excess hydrogen [20]. The introduction of hydrogen has been reported to provide enhanced hydrogen coverage on the film growth surface, allowing incoming  $SiH_3$  to diffuse further to

find more energetically favorable sites. Several research groups have reported that hydrogen acts as an etchant to break weak Si–Si bonds in disordered silicon networks [21]. However, these studies discussed only the reactions on the surface of the growing film, not those in the bulk plasma state. Matsuda *et al* [22] suggested that excess hydrogen affects the gas phase reaction in the bulk plasma by reducing the electron temperature, which is strongly related to the generation of highly reactive radical species. Similarly, in this work, we discussed the reduction of the electron temperature due to hydrogen dilution in terms of the slope  $\Delta\text{Si}^*/\Delta\text{SiH}^*$ .

**Figure 5** shows the  $V_f$  of silicon clusters on silicon films as a function of  $\text{SiH}^*$  intensity under different deposition conditions. The overall trends in the  $V_f$  of silicon clusters were similar to those of the  $\text{Si}^*$  intensity shown in **Figure 4**. This suggested that the slope  $\Delta\text{Si}^*/\Delta\text{SiH}^*$  was roughly correlated with the Si cluster incorporation rate. Thus, the value of  $\Delta\text{Si}^*/\Delta\text{SiH}^*$  could be used as simple indicator to determine cluster-free deposition conditions, although the complex experimental conditions with device characteristics should be further analyzed. As shown in **Figure 5**, under pure silane conditions at 0.2 Torr, more clusters were incorporated into the growing film than under other conditions. This might have been due to a longer mean free path due to the lower operating pressure, higher electron density, and higher deposition rates.

#### 4. Conclusion

We observed the variations in emissive radical species and their contributions to film deposition to investigate the correlation between the slope of the  $\text{Si}^*$  intensity versus the  $\text{SiH}^*$  intensity and the  $V_f$  of Si clusters. As the working pressure was decreased, the slope of the  $\text{Si}^*$  intensity versus the  $\text{SiH}^*$  intensity increased. The slope also increased when the gas flow rate was decreased and the pressure was kept constant. When the silane was diluted with hydrogen but the overall flow rate was kept constant, the resulting slope was smaller than that observed under the pure silane conditions. The relationship between the silicon cluster volume fraction and the  $\text{SiH}^*$  intensity was roughly correlated with the slope of the  $\text{Si}^*$  intensity versus the  $\text{SiH}^*$  intensity. These results suggest that this slope could be a potential indicator for predicting the rate of cluster incorporation into the film.

#### Author Contributions

Conceptualization, Y. W. Kim; Methodology, Y. W. Kim; In-

vestigation, Y. W. Kim; Data curation, Y. W. Kim; Writing-Original Draft Preparation, Y. W. Kim; Writing-Review & Editing, Y. W. Kim; Visualization, Y. W. Kim; Supervision, Y. W. Kim

#### References

- [1] X. P. Yan, "Progress review of new energy application in ship," *Ship & Ocean Engineering*, vol. 39, no. 6, pp. 111-115, 2010.
- [2] Y. S. An, *et al.*, "In situ measurement of shortwave radiation by ship for harvesting sea solar energy," *Journal of the Korean Society of Marine Engineering*, vol. 41, no. 8, pp. 714-722, 2017.
- [3] K. K. Lee, D. H. Doh, U. K. Kim, and H. S. Moon, "A study on market predictions of eco ship's engine and machinery," *Journal of the Korean Society of Marine Engineering*, vol. 38, no. 10, pp. 1354-1359, 2014.
- [4] J. S. Park, M. O. So, and H. H. Yoo, "A study on the operation method of photovoltaic/diesel hybrid generating system," *Journal of the Korean Society of Marine Engineering*, vol. 28, no. 2, pp. 309-314, 2004.
- [5] A. Shah, P. Torres, R. Tscharnner, N. Wyrsh, and H. Keppner, "Photovoltaic technology: the case for thin-film solar cells," *Science*, vol. 285, no. 5428, pp. 692-698, 1999.
- [6] A. Matsuda, "Thin-film silicon-growth process and solar cell application-," *Japanese Journal of Applied Physics*, vol. 43, no.12, pp. 7909-7920, 2004.
- [7] D. L. Staebler and C. R. Wronski, "Reversible conductivity changes in discharge-produced amorphous Si," *Applied Physics Letters*, vol. 31, no. 4, pp. 292-294, 1977.
- [8] K. Shimakawa, A. Kolobov, and S. R. Elliott, "Photoinduced effects and metastability in amorphous semiconductors and insulators," *Advances in Physics*, vol. 44, no. 6, pp. 475-588, 1995.
- [9] K. Koga, N. Kaguchi, M. Shiratani, and Y. Watanabe, "Correlation between volume fraction of clusters incorporated into a-Si:H films and hydrogen content associated with Si-H<sub>2</sub> bonds in the films," *Journal of Vacuum Science & Technology A: Vacuum, Surfaces, and Films*, vol. 22, no. 4, pp. 1536-1539, 2004.
- [10] K. Koga, T. Inoue, K. Bando, S. Iwashita, M. Shiratani, Y. Watanabe, "Highly stable a-Si:H films deposited by using multi-hollow plasma chemical vapor deposition," *Japanese*

- Journal of Applied Physics, vol. 44, no. 11L, pp. L1430-L1432, 2005.
- [11] K. Koga, S. Iwashita, and M. Shiratani, "Transport of nano-particles in capacitively coupled rf discharges without and with amplitude modulation of discharge voltage," *Journal of Physics D: Applied Physics*, vol. 40, no. 8, pp. 2267-2271, 2007.
- [12] F. J. Kampas and R. W. Griffith, "Optical emission spectroscopy: Toward the identification of species in the plasma deposition of hydrogenated amorphous silicon alloys," *Solar Cells*, vol. 2, no. 4, pp. 385-400, 1980.
- [13] B. Drevillon, J. Huc, A. Lloret, J. Perrin, G. de Rosny, and J. P. M. Schmitt, "Silane dissociation mechanisms and thin film formation in a low pressure multipole dc discharge," *Applied Physics Letters*, vol. 37, no. 7, pp. 646-648, 1980.
- [14] S. Nunomura, M. Kita, K. Koga, M. Shiratani, and Y. Watanabe, "In situ simple method for measuring size and density of nanoparticles in reactive plasmas," *Journal of applied physics*, vol. 99, no. 8, p. 083302, 2006.
- [15] M. Takai, T. Nishimoto, M. Kondo, and A. Matsuda, "Chemical-reaction dependence of plasma parameter in reactive silane plasma," *Science and Technology of Advanced Materials*, vol. 2, no. 3-4, pp. 495-503, 2001.
- [16] K. Koga, N. Kaguchi, K. Bando, and M. Shiratani, "Cluster-eliminating filter for depositing cluster-free a-Si:H films by plasma chemical vapor deposition," *Review of Scientific Instruments*, vol. 76, no. 11, p. 113501, 2005.
- [17] Y. W. Kim, K. Koga, and M. Shiratani, "Particle behavior and its contribution to film growth in a remote silane plasma," *Journal of Vacuum Science & Technology A*, vol. 36, no. 5, p. 050601, 2018.
- [18] T. Nishimoto, M. Takai, H. Miyahara, M. Kondo, and A. Matsuda, "Amorphous silicon solar cells deposited at high growth rate," *Journal of Non-Crystalline Solids*, vol. 299, pp. 1116-1122, 2002.
- [19] Y. W. Kim, K. Koga, and M. Shiratani, "Effect of hydrogen dilution on the silicon cluster volume fraction of a hydrogenated amorphous silicon film prepared using plasma-enhanced chemical vapor deposition," *Current Applied Physics*, vol. 20, no. 1, pp. 191-195, 2020.
- [20] S. Guha, J. Yang, D. L. Williamson, Y. Lubianiker, J. D. Cohen, and A. H. Mahan, "Structural, defect, and device behavior of hydrogenated amorphous Si near and above the onset of microcrystallinity," *Applied Physics Letters*, vol. 74, no. 13, pp. 1860-1862, 1999.
- [21] T. Shimizu, "Staebler-Wronski effect in hydrogenated amorphous silicon and related alloy films," *Japanese Journal of Applied Physics*, vol. 43, no. 6R, pp. 3257-3268, 2004.
- [22] A. Matsuda, M. Takai, T. Nishimoto, and M. Kondo, "Control of plasma chemistry for preparing highly stabilized amorphous silicon at high growth rate," *Solar Energy Materials and Solar Cells*, vol. 78, no. 1-4, pp. 3-26, 2003.